XIII International Conference on Computational Plasticity. Fundamentals and Applications
COMPLAS XIII
E. Oñate, D.R.J. Owen, D. Peric and M. Chiumenti (Eds)

SIMILARITY METHODS IN ELASTO-PLASTIC BEAM BENDING

CHRISTIAN ZEHETNER[*], FRANZ HAMMELMÜLLER[*], HANS IRSCHIK[†] AND WOLFGANG KUNZE[X]

[*] Linz Center of Mechatronics (LCM)
Altenbergerstrasse 69, 4040 Linz, Austria
e-mail: christian.zehetner@lcm.at, web-page: www.lcm.at

[†] Institute for Technical Mechanics
Johannes Kepler University
Altenbergerstrasse 69, 4040 Linz, Austria
e-mail: hans.irschik@jku.at – web page: http://www.jku.at/tmech

[X] Salvagnini Maschinenbau GmbH,
Dr. Guido Salvagnini-Strasse 1, 4482 Ennsdorf, Austria
e-mail: wolfgang.kunze@salvagninigroup.com - web page: www.salvagninigroup.com

Key words: plastic bending, similarity methods, drop-test.

Abstract. In industrial metal forming processes a large number of parameters has to be considered. As is well known, this number can be reduced by a non-dimensional representation. Based on the example of an elasto-plastic cantilever beam, the non-dimensional form is derived in the framework of the Bernoulli-Euler theory. In the second step, a Finite Element analyis of a drop-test experiment is performed, and the results are presented in non-dimensional form. The results illustrate the advantage of the normalization.

1 INTRODUCTION

In industrial metal forming processes, high versatility is claimed with respect to material types, geometric dimensions and process parameters. In order to control and optimize the production process, efficient simulation models are required. Usually, metal forming simulation models are very complex and highly non-linear. Thus, parameter studies take a large computational effort. An efficient and practicable way to reduce the number of the essential parameters is the application of non-dimensional formulations, a procedure that finds its theoretical foundation in Similarity Methods [1], [2].

In the following, plastic bending of a cantilever beam is investigated. Especially, the plastic deformations are caused by a drop test as discussed in [1]: A cantilever beam is fixed on a drop mass which is falling down from a predefined height and stopped by an elastic spring, such that the impact causes plastic deformations. In [1] experimental results have been presented with two materials and two configurations of geometric dimensions. Applying the concept of similarity, i.e. the Buckingham Pi Theorem, the number of parameters to describe

the process has been reduced by introducing appropriate normalized quantities.

In the present paper, the non-dimensional representation of the elasto-plastic cantilever beam and the drop-test experiment are investigated in more detail. First, in section 2, the bending process is modelled quasi-statically in the framework of Bernoulli-Euler beam theory assuming a uni-axial state of stress and elasto-plastic material behavior, cf. [5] and [6]. In the latter references ideal plastic material behaviour has been assumed. In the present contribution, the formulation is extended for exponential stress-strain relation of the Ludwik type. With an appropriate normalization of the equilibrium equations, a representation is found in terms of the same non-dimensional quantities as suggested in [1].

Furthermore, in section 3, we discuss the outcomes of a Finite Element model, which we have implemented for the drop test process, using the software package ABAQUS, version 6.12-1. The beam is represented by continuum elements, elasto-plastic material behavior with exponential stres-strain relation is assumed, and large deformation is taken into account. A dynamic analysis is performed in order to simulate the drop-test. With this model, parameter studies have been performed, and the results are represented in terms of the non-dimensional form as suggested in [1]. With the simulation model, a very detailed analysis of the influences of several geometrical and material properties becomes possible.

2 ELASTO-PLASTIC BENDING OF A CANTILEVER BEAM

In the following we consider a cantilever beam with length L as shown in Figure 1. The cross-section of the beam is rectangular with width B and height H. The beam is fixed to a moving rigid base with prescribed acceleration a_z.

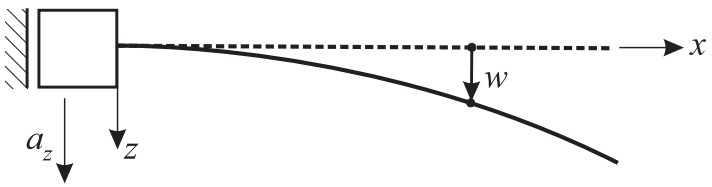

Figure 1: Accelerated cantilever beam

With the density ρ of the beam, the influence of the rigid body acceleration can be represented by a uniform constant distributed transversal load with amplitude

$$q = \rho HBa_z . \tag{1}$$

In the framework of a quasi-static modeling, the moment follows to

$$M = \tfrac{1}{2} q(L-x)^2 . \tag{2}$$

The transversal deflection of a point on the beam axis relative to the base motion is denoted as w. The material behavior is assumed to be elasto-plastic with exponential stress-strain relation of Ludwik's type. For a uni-axial state of stress the constitutive relations read

$$\begin{aligned} \sigma &= E\varepsilon \quad \text{for } \sigma \le \sigma_Y , \\ \sigma &= a\varepsilon^b \quad \text{for } \sigma < \sigma_Y , \end{aligned} \tag{3}$$

where σ is the axial stress, ε the axial strain, E Young's modulus, a and b specify the exponential stress-strain relation, and σ_Y is the yield stress, following from solving Eq. (3),

$$\sigma_Y = E\left(E/a\right)^{1/(b-1)}. \tag{4}$$

2.1 Plastic zones

The bending moment is given by

$$M = B\int \sigma(z) z dz. \tag{5}$$

In the elastic range, the distribution of the stress is linear over the cross-section. The yield moment corresponds to the state where the yield stress is reached at $z=H/2$, i.e. $M_Y = \frac{1}{6}\sigma_Y B H^2$. In the quasi-static case, the yield load follows from Eq. (2) by substituting $x=0$,

$$q_Y = \tfrac{1}{3} B H^2 L^{-2} \sigma_Y. \tag{6}$$

If the load is higher than the yield load, the domain is divided into elastic and plastic zones as shown in Figure 2. Assuming that the deformations remain small and that the Bernoulli-Euler hypothesis holds, the axial strain reads

$$\varepsilon = -z w''. \tag{7}$$

Thus, the stress in the elastic and plastic zones can be expressed by

$$\begin{aligned} \sigma &= \sigma_Y \frac{z}{z_Y} && \text{for } z \le z_Y, \\ \sigma &= a\left(\frac{\sigma_Y}{E}\frac{z}{z_Y}\right)^b && \text{for } z < z_Y. \end{aligned} \tag{8}$$

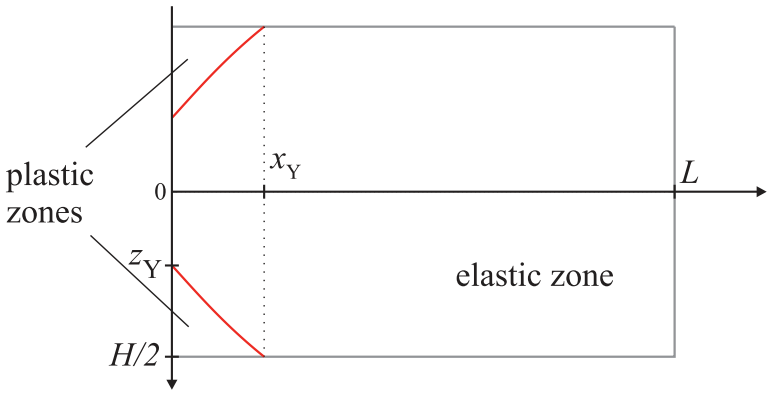

Figure 2: Elastic and plastic zones

The boundary of the plastic zone follows from equating Eqs. (2) and (5), using Eq. (8):

$$2B\left(\int_0^{z_Y}\sigma_Y\frac{z}{z_Y}z\,dz+\int_{z_Y}^{H/2}a\left(\frac{\sigma_Y}{E}\frac{z}{z_Y}\right)^b dz\right)=\tfrac{1}{2}q(L-x)^2. \tag{9}$$

From Eq. (9) the length x_Y of the plastic zone is obtained by substituting $z=H/2$. An analytical solution is possible. On the other hand side, the height z_Y of the plastic zone is obtained as a function of x. Due to the nonlinearity of the equation, z_Y has to be solved numerically.

2.2 Curvature

From Eqs. (3) and (7) follows that

$$\sigma_Y=-Ez_Yw''. \tag{10}$$

Inserting Eq. (10) into Eq. (9) yields an equation for the curvature in the elasto-plastic case:

$$-2B\left(\int_0^{z_Y}Ew''z^2dz+\int_{z_Y}^{H/2}a\left(w''z\right)^b dz\right)=\tfrac{1}{2}q(L-x)^2. \tag{11}$$

Due to the nonlinearity with respect to w'',only a numerical solution is possible. For the elastic range, $x>x_Y$, Eq. (11) simplifies to the well-known form

$$w''=6\frac{q}{BH^3E}(L-x)^2. \tag{12}$$

3.2 Normalization

In order to obtain a generalized representation, a normalization of the above equations has been performed as follows: By introducing the non-dimensional quantities

$$\xi=\frac{x}{L},\quad \zeta=\frac{z}{L},\quad H^*=\frac{H}{L},\quad a^*=\frac{a}{E},\quad q^*=\frac{q}{aB},\quad \sigma^*=\frac{\sigma}{E}, \tag{13}$$

Eq. (9) can be rewritten as

$$2a^{**}\zeta_Y^2(2+b-3a^{**b})+3\left(\frac{1}{2}\right)^{1+b}a^*H^{*2}(a^{**}H^*\zeta_Y^{-1})^b=\frac{3}{2}q^*a^*(\xi-1)^2(2+b) \tag{14}$$

with

$$a^{**}=\left(\frac{1}{a^*}\right)^{\frac{1}{b-1}}. \tag{15}$$

Substituting $\zeta_Y=H^*/2$ and solving Eq. (14) yields the normalized extension ξ_Y of the plastic zone. On the other hand side ζ_Y is obtained as a function of ξ. Figure 3 shows the

solutions for ξ_Y as a function of $Q^* = q^* / q_Y^*$ and $\zeta_Y(\xi)$ for some values of Q^*. Introducing the normalized curvature and deflection

$$w^{*\prime\prime} = Lw'', \quad w^* = \frac{w}{L} \tag{16}$$

Here and in the following the convention is used.

$$w^{*\prime\prime} = \frac{d^2 w^*}{d\xi^2}, \quad w'' = \frac{d^2 w}{dx^2} \tag{17}$$

Substituting Eq. (13) into Eq. (11) yields the equation for the normalized curvature for the elasto-plastic range ($\xi \le \xi_Y$):

$$-\frac{1}{2+b}\left(4w^{*\prime\prime\prime}\zeta_Y^3(2+b)+12a^*\zeta_Y^2\left(-w^{*\prime\prime}\zeta_Y\right)^b-3a^*H^{*2}\left(-\frac{1}{2}w^{*\prime\prime}H^*\right)^b\right)=3q^*a^*(\xi-1)^2 \tag{18}$$

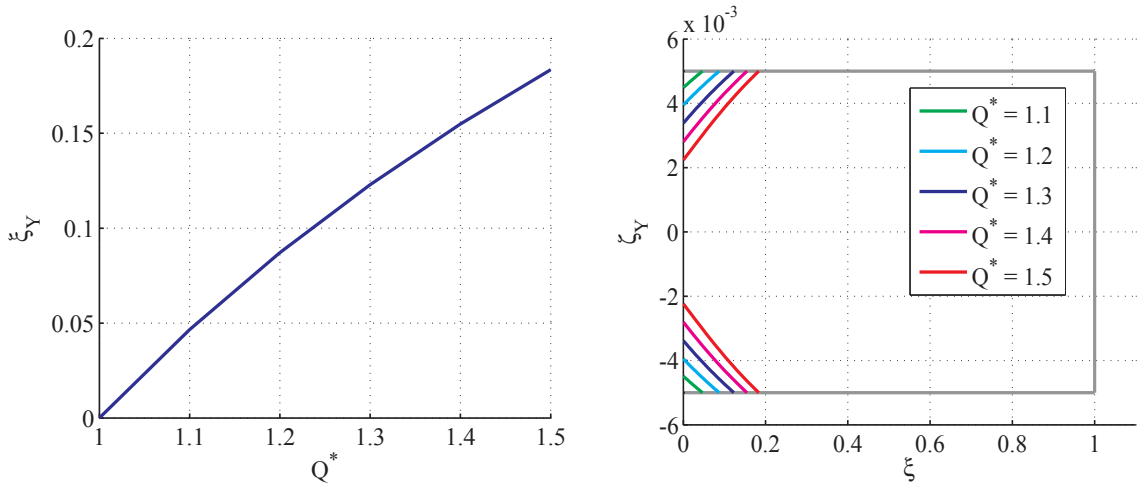

Figure 3: (a) Extension of the plastic zone, (b) Boundary of the plastic zone

Substituting Eqs. (13) and (16) into Eq. (12) yields the normalized curvature for the elastic range ($\xi > \xi_Y$)

$$w^{*\prime\prime} = 6\frac{q^* a^*}{H^{*3}}(\xi-1)^2. \tag{19}$$

Solving Eq. (18) numerically yields the curvature as a function of ξ as shown in Figure 4a. Numerical integration of Eqs. (18) and (19) provides the deflection as shown in Figure 4b.

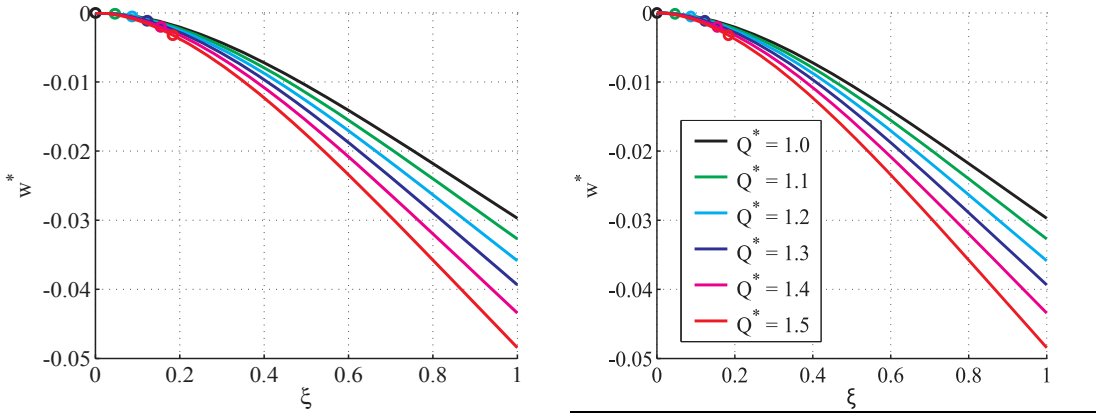

Figure 4: Results for (a) Curvature and (b) Deflection

Figure 5a shows the plastic tip displacement as a function of the rigid body acceleration a_z. The rigid-body acceleration at first yield is denoted as $a_{z,Y}$ which is obtained by inserting Eq. (6) into Eq. (1). In this dimensional representation, for each configuration of H and L a separate curve is obtained. However, in the non-dimensional representation in Figure 5b, only one curve is obtained for the three cases.

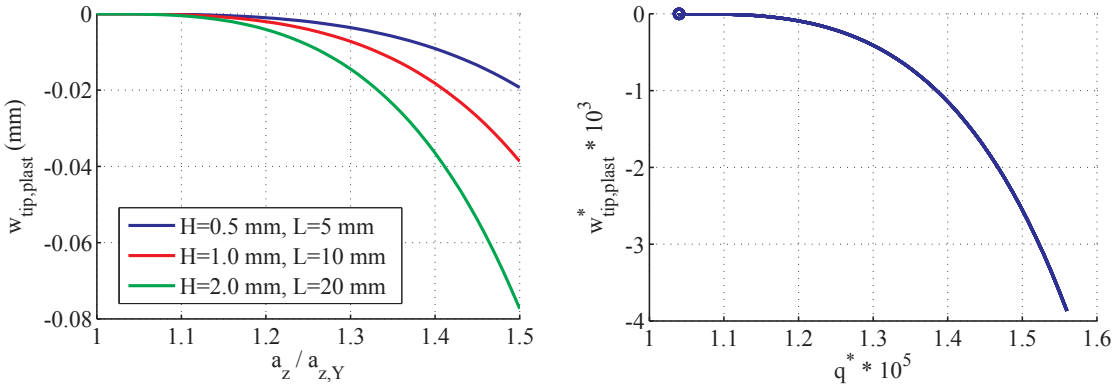

Figure 5: Plastic tip displacement (a) dimensional and (b) non-dimensional representation

2.3 Discussion of the non-dimensional formulation

In the dimensional representation with the coordinates x and z, the bending process is specified by eight physical quantities:

$$w, a_z, E, a, b, H, L, \rho. \tag{20}$$

On the other hand, in the dimensionless formulation derived in section 2.2 with the normalized coordinates $\xi = x/L, \quad \zeta = z/L$ the number of essential parameters has been reduced to five non-dimensional quantities

$$\frac{w}{L}, \frac{\rho a_z H}{a}, \frac{a}{E}, b, \frac{H}{L}. \tag{21}$$

The results show that for the simple model of an elasto-plastic beam bending process the same normalized quantities have been derived as have been obtained by Baker et al. [1] using the Buckingham Pi theorem.

Recall that all the results in this section are based on the geometrically linear Bernoulli-Euler beam theory with exponential stress-strain relation. Thus the results are valid for small deformations. Goal of this section has been an analytic derivation of the non-dimensional formulation. In the next section, the drop test as presented in [1] is simulated by means of Finite Element computations, considering large deformations. The results are expressed in terms of the same non-dimensional form.

3 FINITE ELEMENT SIMULATION OF THE DROP-TEST

3.1 Simulation model

Figure 6 shows the drop-test as discussed in [1]. A cantilever beam is fixed on a drop mass. At the cantilever tip an additional beam with higher thickness is attached. The length of the cantilever is L, and H_D is the drop height.

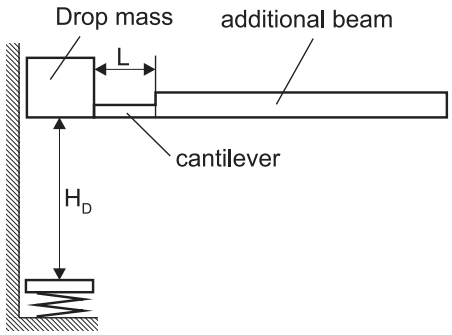

Figure 6: Drop-test

For this setup a Finite Element model has been implemented as follows: The drop mass is modelled as a rigid body, and the beam by three-dimensional Finite Elements. A dynamic analysis is performed to model the complete drop-test. After falling down and colliding with the spring the cantilever beam deforms due to inertial forces. Two kinds of beams are considered with the properties according to Table 1.

Table 1: Parameters

			Beam 1	Beam 2
Cantilever	length	mm	12.7	25.4
	height	mm	0.508	1.016
	width	mm	6.35	12.7
Additional beam	length	mm	114.3	228.6
	height	mm	1.016	2.032
	width	mm	6.35	12.7
Material	type		Steel	Aluminium
	Young's modulus	N/m²	2.068e11	6.895e10
	yield stress	N/m²	2.30e8	1.15e8
	density	kg/m^3	7805.73	2740.31
Drop mass	weight of drop mass	kg	0.767	3.8147

3.2 Numerical results

Figure 7 shows the deformed configuration after the impact of the drop mass with the spring.

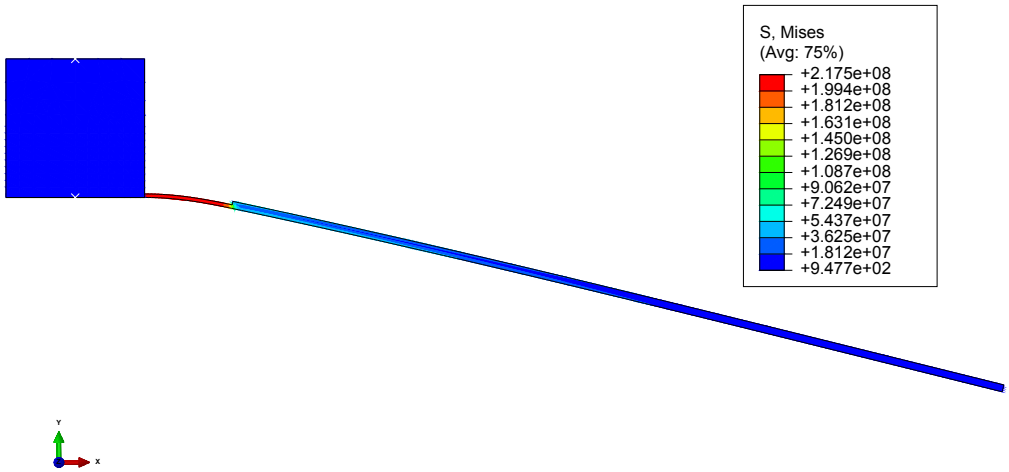

Figure 7: Deformed configuration after impact with spring

The time response of the transversal displacement is shown in Figure 8. The deformation of the cantilever consists of the plastic part with super-imposed elastic vibrations. In Figure 8 the maximum deflection and the plastic part are marked.

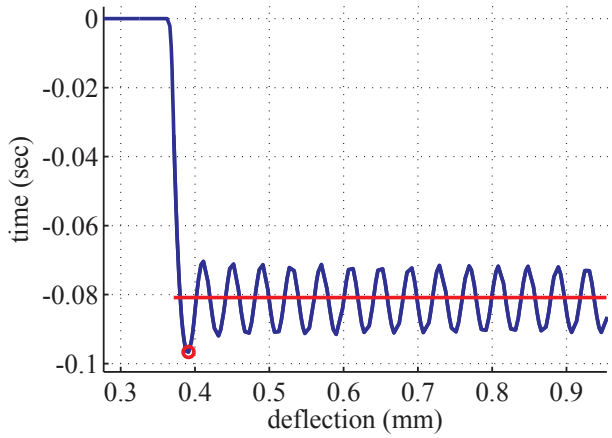

Figure 8: Transversal displacement

Figure 9 shows the maximum deflection and the plastic deflection as a function of the drop height H_D. In this dimensional representation the deflection of the aluminium beam is larger than the deflection of the steel beam. On the other hand side, Figure 10 shows the non-dimensional deflection w^* as a function of the non-dimensional drop height H_D^*, given by

$$H_D^* = \frac{\rho g H}{\sigma_Y}, \quad w^* = \frac{w}{L}. \tag{22}$$

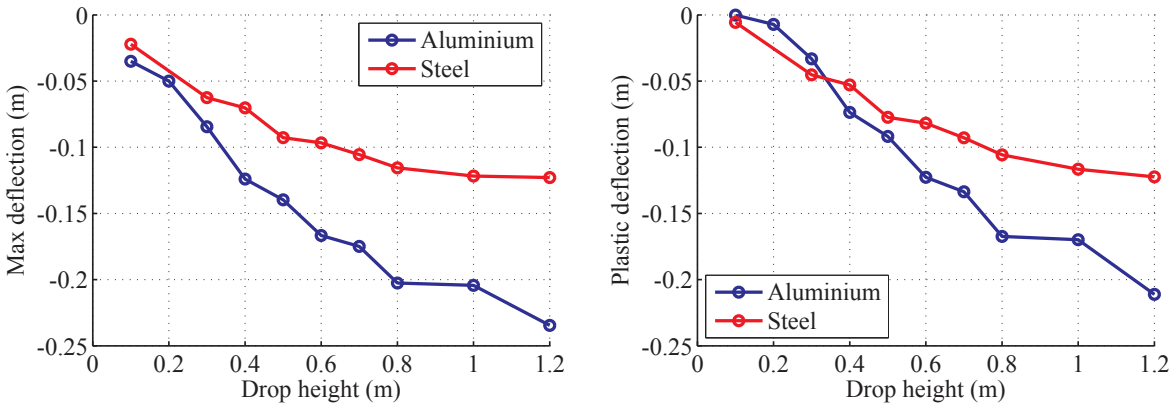

Figure 9: (a) Maximum deflection and (b) plastic deflection

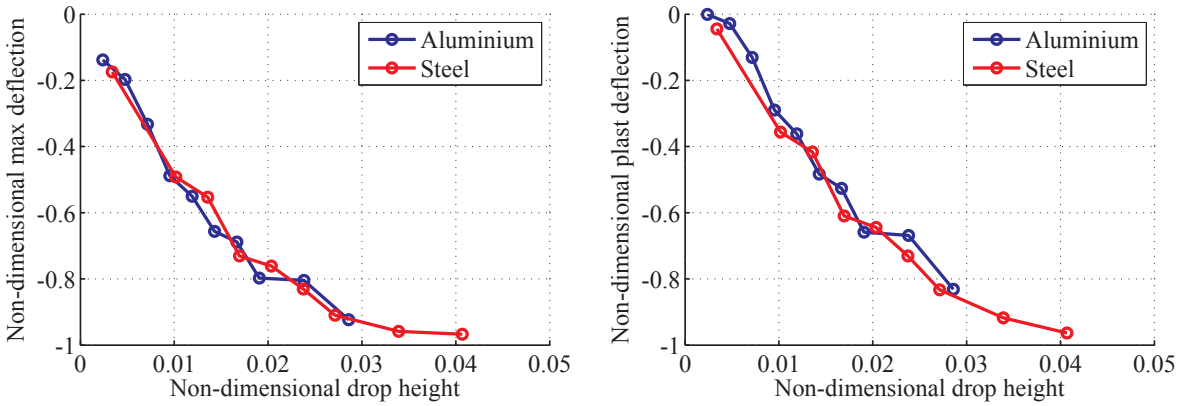

Figure 10: (a) Maximum deflection, (b) Plastic deflection

In this normalized representation, the non-dimensional deflection is equal for both beams, as it has been shown in the experimental drop-test in [1]. From the investigations in section 2 it follows that one curve is obtained for equal relations of the non-dimensional parameters a/E, b and H/L. In the present case, the ratio H/L is the same for both beams. The exponent b and the ratio a/E are differing slightly for aluminium and steel. However, this influence is negligible. Note that the result for a differing ratio H/L would be another curve in the non-dimensional representation.

4 CONCLUSIONS

A non-dimensional representation of the elasto-plastic bending process has been derived in the framework of Bernoulli-Euler beam theory. It has been shown how the number of parameters can be reduced by a non-dimensional formulation. In the second step, a Finite Element simulation has been performed for a drop-test. In the non-dimensional representation, the results for the steel and aluminium beam coincide. The results coincide with [1], where the non-dimensional quantities have been derived by the Buckingham Pi theorem, and applied to

an experimental drop test. The results show that in complex industrial problems the computational effort for numerical simulations and parameter studies can be reduced significantly by applying appropriate normalization strategies.

REFERENCES

[1] Baker, W.E., Westine, P.S., and Dodge, F.T. Similarity Methods in Engineering Eynamics, Theory and Practice of Scale Modeling, Elsevier (1991).
[2] Sedov, L.I. Similarity and Dimensional Methods in Mechanics, CRC Press (1993).
[3] Szabó, I. Höhere Technische Mechanik, Springer (2001).
[4] Ziegler, F. Mechanics of Solids and Fluids, Springer (2005).
[5] Yu, T.X., and Zhang, L.C. Plastic Bending, Theory and Applications, World Scientific (1996).
[6] Natarajan, A. and Peddieson, J. Simulation of beam plastic forming with variable bending moments, International Journal of Non-Linear Mechanics (2011), 46: 14-22.